Histol Histopathol (2023) 38: 709-724

https://www.hh.um.es

Histology and Histopathology
From Cell Biology to Tissue Engineering

ORIGINAL ARTICLE **Open Access**

CircRNA hsa_circ_0075048 promotes the malignant progression of non-small cell lung cancer by up-regulating HMGB2 expression via targeting miR-1225-5p

Jijiong Zhang[1,2] and Jinjuan Mao[1,2]

[1]Department of Respiratory Medicine, Huangshi Central Hospital, Affiliated Hospital of Hubei Polytechnic University, Edong Healthcare Group, Huangshi and [2]Hubei Key Laboratory of Kidney Disease Pathogenesis and Intervention, Hubei, PR China

Summary. Background. Non-small cell lung cancer (NSCLC) is one of the most common forms of lung cancer. Circular RNAs (circRNAs) have been recognized that can be used as novel molecular markers for cancer therapy. Here, we attempted to identify the role of hsa_circRNA_0075048 (circ_0075048) in NSCLC.

Methods. Quantitative real-time polymerase chain reaction (qRT-PCR) was performed to analyze the levels of hsa_circ_0075048, miR-1225-5p and high mobility group box-2 (HMGB2). Cell proliferation was detected by Cell Counting Kit 8 (CCK8) and 5-Ethynyl-2'-deoxyuridine (EdU) assays. Flow cytometry was used to detect apoptosis. Transwell assay was used to assess cell migration and invasion. Sphere formation ability was tested by cell pellet test. The protein expression levels were detected by western blot and immunohistochemistry. Dual-luciferase reporter assay, RNA-pull down and RNA immunoprecipitation (RIP) assays were used to verify the targeting relationships between miR-1225-5p and circ_0075048 or HMGB2. Mice tumor models were constructed to ascertain the effects of circ_0075048 on tumor growth *in vivo*.

Results. Circ_0075048 was increased in NSCLC tissues and cells. NSCLC cell proliferation, migration, invasion and sphere formation ability were decreased by circ_0075048 knockdown, and cell apoptosis was induced. Downregulation of miR-1225-5p recuperated the effects of circ_0075048 knockdown on NSCLC progression. The effects of miR-1225-5p on cell proliferation, apoptosis, migration, invasion and sphere formation were attenuated by HMGB2 overexpression.

Conclusion. This study indicated that circ_0075048 played an oncogenic role in the development of NSCLC by regulating miR-1225-5p and HMGB2. The data provide more possibilities for the treatment of NSCLC.

Key words: circ_0075048, miR-1225-5p, HMGB2, Non-small cell lung cancer

Corresponding Author: Jinjuan Mao, Department of Respiratory Medicine, Huangshi Central Hospital, Affiliated Hospital of Hubei Polytechnic University, Hubei Key Laboratory of Kidney Disease Pathogenesis and Intervention, No.141 Tianjin Road, Huangshi 435000, China. e-mail: mjj20210312@163.com

DOI: 10.14670/HH-18-551

Introduction

Lung cancer, a malignant tumor originating primarily in the bronchus or alveoli, is one of the leading causes of death in both men and women (Siegel and Miller, 2019), that includes non-small cell lung cancer (NSCLC, 80%) and small cell lung cancer (Planchard et al., 2018). With the progress of medicine, great breakthroughs have been made in the treatment of NSCLC (Forde et al., 2018), but the clinical results of advanced lung cancer are still unsatisfactory (Chen et al., 2020). Therefore, further understand of the pathogenesis of NSCLC is crucial for developing new and effective clinical treatment for NSCLC patients.

Molecular marker technology has become an important means of tumor therapy and diagnosis, and increasing research has indicated that circular RNAs (circRNAs) act as molecular markers for cancer therapy. CircRNAs are a group of RNAs characterized by covalently closed loop structures lacking terminal 5' caps and 3' polyadenylated tails, so they have greater stability than linear RNA and can be resistant to the degradation of RNase R exonucleases (Arnaiz et al., 2019). Jiao et al. confirmed that hsa_circ_0000745 was the tumor promoter of cervical cancer (CC), the results of functional tests showed that overexpression of hsa_circ_0000745 notably expedited CC cell growth (Jiao et al., 2020). Circ-CAP4 were substantially reinforced in NSCLC cells and tissues, and down-regulation of circ-CPA4 inhibited cell growth and promoted NSCLC cell death (Hong et al., 2020). CircPTK2 was significantly down-regulated in NSCLC cells, and overexpression of circPTK2 inhibited the

metastasis of NSCLC cells (Wang et al., 2018). However, hsa_circ_0075048 (circ_0075048) in NSCLC has not been reported.

MicroRNAs (miRNA/miR), about 25 bp in length, are not directly in the protein synthesis of organisms (Chaudhuri and Chatterjee, 2007). It has been reported that miRNAs are associated with drug resistance and prognosis of cancer patients as well as the growth and development of cancer cells (Tutar, 2014). It has been reported that miR-1225-5p acted as a cancer suppressor in a variety of tumors, such as glioblastoma (Wang et al., 2020), osteosarcoma (Zhang et al., 2020) and laryngeal cancer (Sun et al., 2019) and so on. Li et al. showed that miR-1225-5p in NSCLC tissues and cells was apparently down-regulated and negatively correlated with NSCLC proliferation (Li et al., 2020). However, the role and regulatory relationship in NSCLC between miR-1225-5p and circ_0075048 are unclear.

High mobility group box-2 (HMGB2), a member of the HMGB family, is distributed in testis and lymphoid tissues, and HMGB2 was evidently augmented in gastric cancer (GC) tissues, which was negatively correlated with the prognosis of GC (Fang et al., 2020). HMGB2 was greatly expressed in breast cancer (BC) cells, down-regulation of HMGB2 expression could evidently hamper the growth and glycolysis of BC cells (Fu et al., 2018). It had been reported that HMGB2 was highly expressed in NSCLC tissues and played an oncogenic role (Zhou et al., 2019). Overexpression of HMGB2 was associated with lymph node metastasis and advanced tumor node metastasis (TNM) in NSCLC (Lou et al., 2022). However, the role of the circ_0075048/miR-1225-5p/HMGB2 axis in NSCLC is unclear and needs more research.

This study explored the functions of circ_0075048 in NSCLC for the first time and confirmed the regulatory mechanism of has_circ_0075048 in NSCLC. The research opens up new possibilities for the clinical treatment of NSCLC.

Materials and methods

Human samples

64 pairs of NSCLC tissues and adjacent normal tissues were gathered from Huangshi Central Hospital, Affiliated Hospital of Hubei Polytechnic University. All patients offered informed consent. These clinical tissues were placed in liquid nitrogen after they were separated. According to the expression level of circ_0075048 in NSCLC patients, patients were divided into high circ_0075048 expression group and low circ_0075048 expression group. The study was approved by the Ethics Committee of Huangshi Central Hospital, Affiliated Hospital of Hubei Polytechnic University.

Cell lines and cell culture

A549, H1299, H1755, H520 and BEAS-2B cell lines were purchased from Cellcook Biotech Co., Ltd. (Guangzhou, China). All cells were cultured in RPMI-1640 medium (BIOSUN, Shanghai, China) with 10% fetal bovine serum (FBS; Zhejiang Tianhang Biotechnology Co., Ltd., Hangzhou, China) and 1% double solution resistance (penicillin and streptomycin mixture; HyClone Company, Logan, UT, USA).

Quantitative real-time polymerase chain reaction (qRT-PCR)

MiRNeasy Mini Kit (Qiagen, Valencia, CA, USA) was utilized to isolate RNA, and the concentration of RNA was tested. Then isolated RNAs were reverse transcribed into cDNAs using by miScript RT Kit (TaKaRa, Dalian, China). QRT-PCR was performed using miScript SYBR Green PCR Kit (Qiagen) in the ABI Prism 7700 Sequence Detection System (Thermo Fisher Scientific, Rockville, MD, USA). The relative expression level was compared to the expression of glyceraldehyde 3-phosphate dehydrogenase (GAPDH) (circ_0075048, ERGIC1 and HMGB2) or U6 (miR-1225-5p) using the $2^{-\Delta\Delta CT}$ method (Livak and Schmittgen, 2001). Primer sequences are shown in Table 1.

First, for all test and calibration (control) samples, the CT values of reference genes were used to normalize the CT values of target genes.

ΔCT(test) = CT(target, test) - CT(ref, test)

ΔCT(calibrator) = CT(target, calibrator) - CT(ref, calibrator)

Secondly, the ΔCT value of the calibration sample was used to normalize the ΔCT value of the test sample.

ΔΔCT = ΔCT(test) - ΔCT(calibrator)

Finally, the expression level ratio was calculated.

$2^{-\Delta\Delta CT} = 2^{-(\Delta CT(test) - \Delta CT(calibrator))}$

Actinomycin D assay

A549 and H1299 cells were added with 2 μg/mL actinomycin D (Abcam, Cambridge, England) or dimethyl sulfoxide (DMSO; Sigma, St. Louis, MO, USA) to inhibit transcription for 0h, 4h, 8h, 12h and 16h.

Table 1. Sequences used for RT-qPCR.

Name	Primers sequences for PCR (5'-3')	
hsa_circ_0075048	Forward	ATCCCGCTGAACAATGGGG
	Reverse	ACTGACGTCGATCTTGCCAC
HMGB2	Forward	GCACCAGGCAAGAATACCCT
	Reverse	TCCGCGAAATTGACGGAAGA
miR-1225-5p	Forward	GCCGAGGTGGGTACGGCCCA
	Reverse	CTCAACTGGTGTCGTGGA
ERGIC1	Forward	GCACGATGCCCTTTGACTTC
	Reverse	CTCGCAGTGCAGATTGGGTA
GAPDH	Forward	TCCCATCACCATCTTCCAGG
	Reverse	GATGACCCTTTTGGCTCCC
U6	Forward	CTCGCTTCGGCAGCACATATACT
	Reverse	ACGCTTCACGAATTTGCGTGTC

The contents of circ_0075048 and endoplasmic reticulum-golgi intermediate compartment 1 (ERGIC1) mRNA were inspected by qRT-PCR.

RNase R assay

For circ_0075048 stability assay, circ_0075048 and ERGIC1 mRNA expression were measured after treating with or without 10 μL RNase R (Geneseed Biotech Co., Ltd., Guangzhou, China).

CircRNA subcellular localization assay

Cytoplasmic and nuclear RNA in A549 and H1299 cells were separated by Nuclear and Cytoplasmic Extraction Reagents (Thermo Fisher Scientific). Then, data were analyzed by qRT-PCR. GAPDH and U6 were housekeeping genes in cytoplasm and nucleus, respectively.

Cell transfection

To overexpress or limit the expression of HMGB2, miR-1225-5p and circ_0075048, overexpression vectors (HMGB2 and miR-1225-5p) or low expression vectors (anti-miR-1225-5p and sh-circ_0075048#1, sh-circ_0075048#2, sh-circ_0075048#3) and controls (empty vectors and miR-NC, anti-miR-NC) were offered by Nanjing Kebai Biological Technology Co., Ltd. (Nanjing, China). A549 and H1299 cells were seeded in 96-well plates or 6-well plates, and transfected with vectors with the help of LipoGene™ 2000 PLus Transfection Reagent (Suzhou Yuhengsheng Material Technology Co., Ltd., Suzhou, China), and the transfection efficiencies were inspected by qRT-PCR or western blot.

Cell proliferation assay

Cell Counting Kit 8 (CCK8) assay was performed using Cell Counting Kit-8 kit (CCK-8; GLPBIO, Montclair, California, USA) to detect cell viability. 5-Ethynyl-2'-deoxyuridine (EdU) assay was performed according to the directions of YF®488 Click-iT EdU Imaging Kits (Suzhou Yuhengsheng Material Technology Co., Ltd.) to monitor cell proliferation.

Cell apoptosis

A549 and H1299 cells transfected with sh-circ_0075048#1 or sh-NC were collected and resuspended in PBS and 200 μL binding buffer (Beijing BLKW Biotechnology Co., Ltd., Beijing, China), and then tinted with 10 μL Annexin V-FITC (Beijing BLKW Biotechnology Co., Ltd.) at 4°C for 30 min in the dark. Cells were added with 300 μL Binding buffer and strained with a 200-mesh sieve. Finally, cells were appended with 5 μL PI (BLKW) and the apoptosis of cells was measured within one hour using a Cytoflex flow cytometry (Agilent, Beijing, China).

Transwell assay

The migration and invasion abilities of A549 and H1299 cells were assessed with 24-well transwell chambers (Corning, Tewksbury, MA, USA) coated without or with matrigel (BD Biosciences, Franklin Lakes, NJ, USA), respectively. 2×10^6 cells were blended with medium free of serum and added into the upper chamber, and we added the appropriate amount of RPMI-1640 medium including 10% FBS to the lower chamber. Then the migrating or invading cells were fixed and dyed with crystal violet (Solarbio, Beijing, China) at room temperature, and enumerated with a microscope (Olympus, Tokyo, Japan).

Caspase 3 activity determination

Caspase 3 activity was determined with the Caspase Colorimetric Assay Kit (Keygen Biotech, Nanjing, China) following the manufacturer's protocol. Briefly, collected A549 and H1299 cells were washed in PBS, lysed in the provided lysis buffer, followed by centrifuging for 10 min at 4°C. The protein concentration of the supernatant was assayed. Then 150 μg of cell lysate were mixed with Caspase substrate and reaction buffer at 37°C for 2h incubation. Absorbance values were recorded on a microplate reader at 400 nm.

Cell pellet test

Cell precipitates were collected with trypsin (Biological Industries, Kibbutz Beit Haemek, Israel) and PBS (Biological Industries), and cells were mixed in stem cell culture medium. 5×10^4 cells were fostered into the ultra-low adsorption cell culture six-well plates, and the pellet formation status was observed 10 days later.

Western blot

The transfected A549 and H1299 cells in plates were washed with PBS, and collected with cell scraper. The cells were centrifuged to collect the sediment. 300 μL RIPA Lysis Buffer (RIPA: PMSF: phosphatase inhibitors=100:1:1, Beyotime Biotechnology, Jiangsu, China) was added to the precipitate and lysed on ice for half an hour. After lysing, cells were centrifuged at 4°C for 10 min at high speed, and the supernatant was collected.

The standard BSA protein (Beyotime Biotechnology) was diluted to 0.5 mg/mL. BCA working solution was prepared by mixing reagent A and B (Beyotime Biotechnology) at a 50:1 ratio. The standard protein was added to the 96-well plates in gradient dilution, and 200 μL BCA working solution was added to the standard and sample wells, and the mixtures were incubated at 37°C for 1 hour. The OD value at 562 nm of each well was determined by the microplate reader

(Tecan, Mannedorf, Swiss), the protein standard curve was drawn with Excel and the protein concentration of the sample was calculated.

SDS-PAGE Kit (Shanghai Guduo Biological Technology Co., Ltd., Shanghai, China) was used for protein separation. The protein was transferred to the polyvinylidene fluoride (PVDF) membrane (Millipore, Billerica, MA, USA), and then sealed with 5% albumin from chicken egg white (Solarbio). PVDF membrane was hatched with anti-proliferating cell nuclear antigen (PCNA) (1:500, bs-2006R, Bioss, Beijng, China), anti-Cleaved-caspase 3 antibody (1:500, ab32042, Abcam), anti-matrix metallopeptidase 9 (MMP9) (1:500, bs-4593R, Bioss), anti-organic cation/carnitine transporter 4 (OCT4) (1:500, bsm-52002R, Bioss), anti-β-actin (1:5000, bs-0061R, Bioss), anti-HMGB2 antibody (1:10,000, ab124670, Abcam) and Goat Anti-Rabbit IgG H&L/HRP antibody (1:5000, bs-40295G-HRP, Bioss), and was developed by ECL chemiluminescence (Millipore) and photographed in a gel imaging analyzer (UVITEC, Cambridge, England).

Dual-luciferase reporter assay

The circ_0075048-WT and HMGB2-3'UTR-WT were the wild-type sequences of circ_0075048 and HMGB2-3'UTR containing miR-1225-5p target sites, while circ_0075048-MUT and HMGB2-3'UTR-MUT were the mutant-type sequences of circ_0075048 and HMGB2-3'UTR containing the site mutation of miR-1225-5p target sites. PGL3 with circ_0075048 or HMGB2 (circ_0075048-WT, circ_0075048-MUT, HMGB2-3'UTR-WT and HMGB2-3'UTR-MUT) was built by Weston Biomedical Technology Co., Ltd. (Chongqing, China) to perform dual-luciferase reporter assay. These plasmids were transfected into A549 and H1299 cells with miR-1225-5p or miR-NC, respectively. The cells were gathered and operated with dual luciferase reporter assay kit (Promega, Madison, WI, USA) to detect the luciferase activity.

RNA-pull down assay

The biotin-labeled probes for miR-1225-5p (Bio-miR-1225-5p) and its control (Bio-NC) were made by Sangon (Shanghai, China), and then incubated with cell lysate and magnetic beads to form RNA-bead complex, and the binding ability of miR-1225-5p to circ_0075048 was detected by qRT-PCR via detecting circ_0075048 level.

RNA immunoprecipitation (RIP) assay

A549 and H1299 cells were lysed with RIP kit (Millipore), and cultivated with Ago2 antibody (ab186733, Abcam) or IgG antibody (bs-0297P, Bioss) with magnetic beads. Two hours later, the RNA was isolated by miRNeasy Mini Kit (Qiagen), and operated with the qRT-PCR procedure to ensure the expression of circ_0075048 and miR-1225-5p in cells.

Immunohistochemistry (IHC) assay

IHC was used to evaluate the protein expression of HMGB2, Cleaved-caspase3 and Ki-67 in tumor tissues. Tumor tissues were made into 5 μm paraffin sections, which were cultured with anti-HMGB2 (1:100, bs-18052R, Bioss), Cleaved-Caspase 3 (1:100, AF7022, Affinity Nanjing, China) or anti-Ki67 (1:100, bs-23103R, Bioss), and then incubated with secondary antibody (1:1000, ab6721, Abcam). The incubation with PBS served as negative control. 3,3-diaminobenzidine (Solarbio) was chosen to stain sections and the protein expression was evaluated with a microscope (Olympus).

In vivo experiment in mice

Six germ-free mice (Vital River Laboratory Animal Technology, Beijing, China) with similar growth conditions were divided into two groups (n=3/group), and in each group mice were subcutaneously transfected with H1299 cells expressing sh-NC or sh-circ_0075048 to construct mice tumor models. The size of tumors was detected weekly until the fifth week, and the volume was calculated by $0.5\times length\times width^2$. The mice were euthanized, and the tumors were weighed. The animal experiments were approved by the Animal Welfare and

Table 2. Correlation between circ_0075048 expression and clinicopathological features in NSCLC patients.

Characteristics	Circ_0075048 expression	
	High (n=32)	Low (n=32)
Age (year)		
<50	18	15
≥50	14	17
Gender		
Female	16	14
Male	16	18
Tumor size (cm)		
<5	10	19
≥5	22	13
Histology		
Adenoma	21	13
Squamous	11	19
Differentiation		
Moderate-Poor	20	15
Well	12	17
TNM stage		
I+II	7	20
III+IV	25	12
Lymph node metastasis		
Absence	13	15
Presence	19	17

*$P<0.05$.

Research Ethics Committee of Huangshi Central Hospital, Affiliated Hospital of Hubei Polytechnic University.

Statistical analysis

Data were analyzed with SPSS 17.0 (IBM, Chicago, IL, USA) and GraphPad Prism 8.0 software (GraphPad Inc., LaJolla, California, USA). The differences in data were analyzed by the Student's t-test or one-way analysis of variance (ANOVA). Pearson's correlation analysis identified the linear correlation among circ_0075048, miR-1225-5p and HMGB2. Data were presented as mean ± standard deviation, and $P<0.05$ meant significant difference.

Results

Circ_0075048 was highly expressed in NSCLC tissues and cells

As shown in Fig. 1A,B, the differential expression of circRNAs in NSCLC tissues and non-cancer tissues were screened by GEO database (GSE158695), and it was found that circ_0075048 was highly expressed in NSCLC tissues. Circ_0075048 was prominently increased in NSCLC tissues compared with the normal tissues (Fig. 1C). Then patients were grouped into a high circ_0075048 group and a low circ_0075048 group based on the median level of circ_0075048 (3.69), thereafter, the Kaplan-Meier analysis revealed that

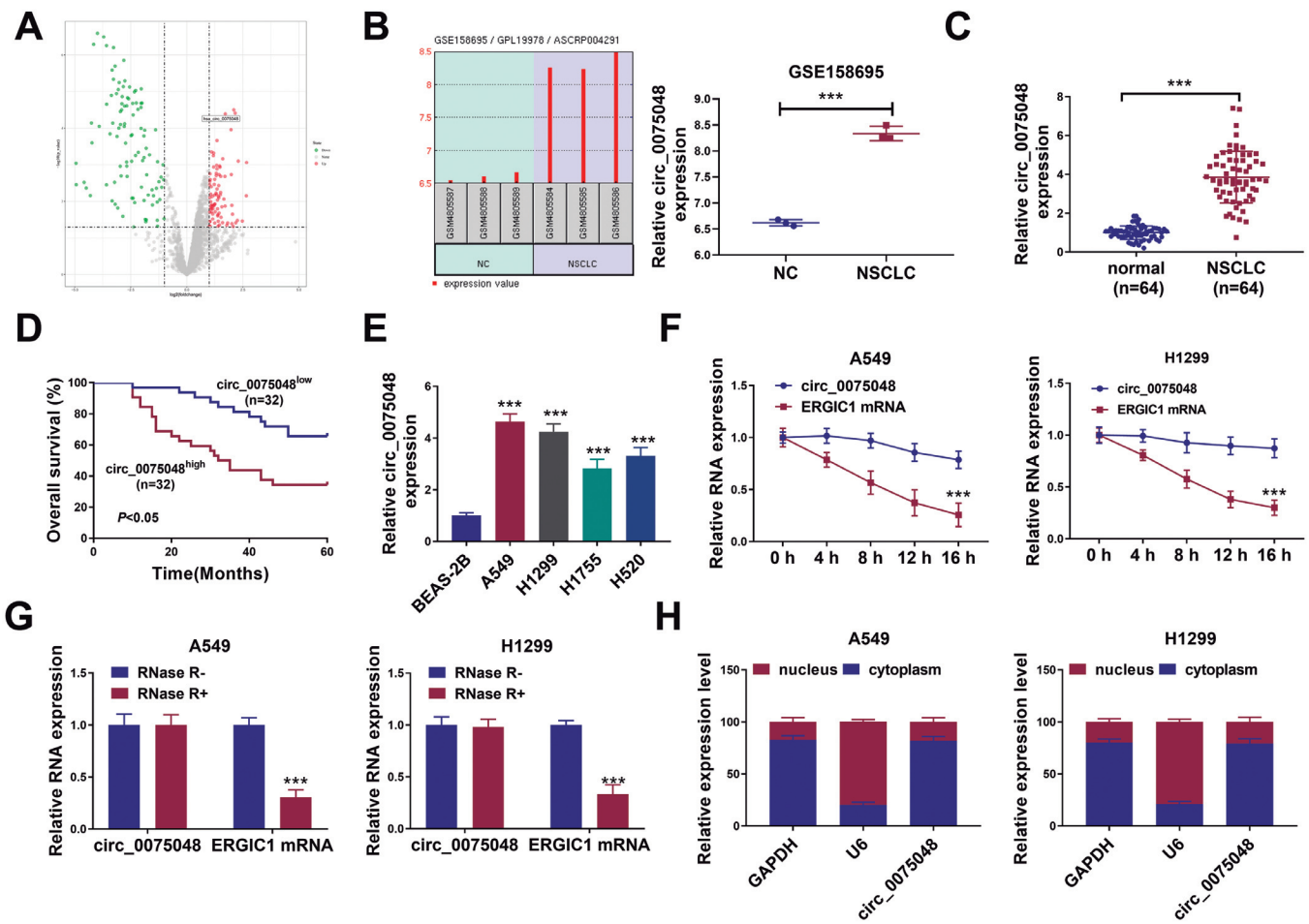

Fig. 1. Circ_0075048 was enhanced in NSCLC tissues and cells. **A.** A volcano plot filtered out the dysregulated genes. Red and green dots denote upregulated and downregulated genes, respectively. **B.** Circ_0075048 expression in NSCLC in the GSE158695 chip was detected. **C.** The content of circ_0075048 in tumor tissues was measured by qRT-PCR. **D.** The overall survival rate in NSCLC patients was evaluated using Kaplan-Meier overall survival curve. **E.** QRT-PCR was hused to test the expression of circ_0075048 in NSCLC cells. **F.** Relative RNA levels of circ_0075048 and ERGIC1 were analyzed by qRT-PCR after treatment with Actinomycin D every 4h in A549 and H1299 cells. **G.** QRT-PCR was used to analyze circ_0075048 and ERGIC1 mRNA levels in A549 and H1299 cells treated with RNase R. **H.** CircRNAs subcellular localization experiment was performed to locate circ_0075048. The cytoplasmic control was GAPDH, while U6 was used as a nuclear control. ***$P<0.001$.

NSCLC patients with high circ_0075048 expression had significantly poorer overall survival as compared to those with low circ_0075048 expression (Fig. 1D). Besides that, higher circ_0075048 expression was correlated with advanced TNM stages and tumor size (Table 2). Univariate analysis showed that the difference in overall survival caused by tumor size, lymph node metastasis, TNM stage or circ_0075048 expression was statistically significant; multivariate analysis suggested that lymph node metastasis and TNM stages both represented independent factors related to the overall survival of patients involved (Table 3). Next, compared to the normal cells, circ_0075048 was up-regulated in NSCLC cells, among them, the two cell lines with the highest expression of circ_0075048 were A549 and H1299 cells (Fig. 1E). Then we performed actinomycin D and RNase R assays in the two cells to verify the circular characteristics of circ_0075048, and the results showed that circ_0075048 was more stable than linear ERGIC1 (Fig. 1F,G). CircRNA subcellular localization in A549 and H1299 cells exhibited that circ_0075048 was mainly expressed in the cytoplasm (Fig. 1H). In short, circ_0075048 was up-regulated in NSCLC tissues and cells.

Knockdown of cic_0075048 inhibited NSCLC cell progress

The transfection efficiency of sh-circ_0075048#1, sh-circ_0075048#2 and sh-circ_0075048#3 were tested

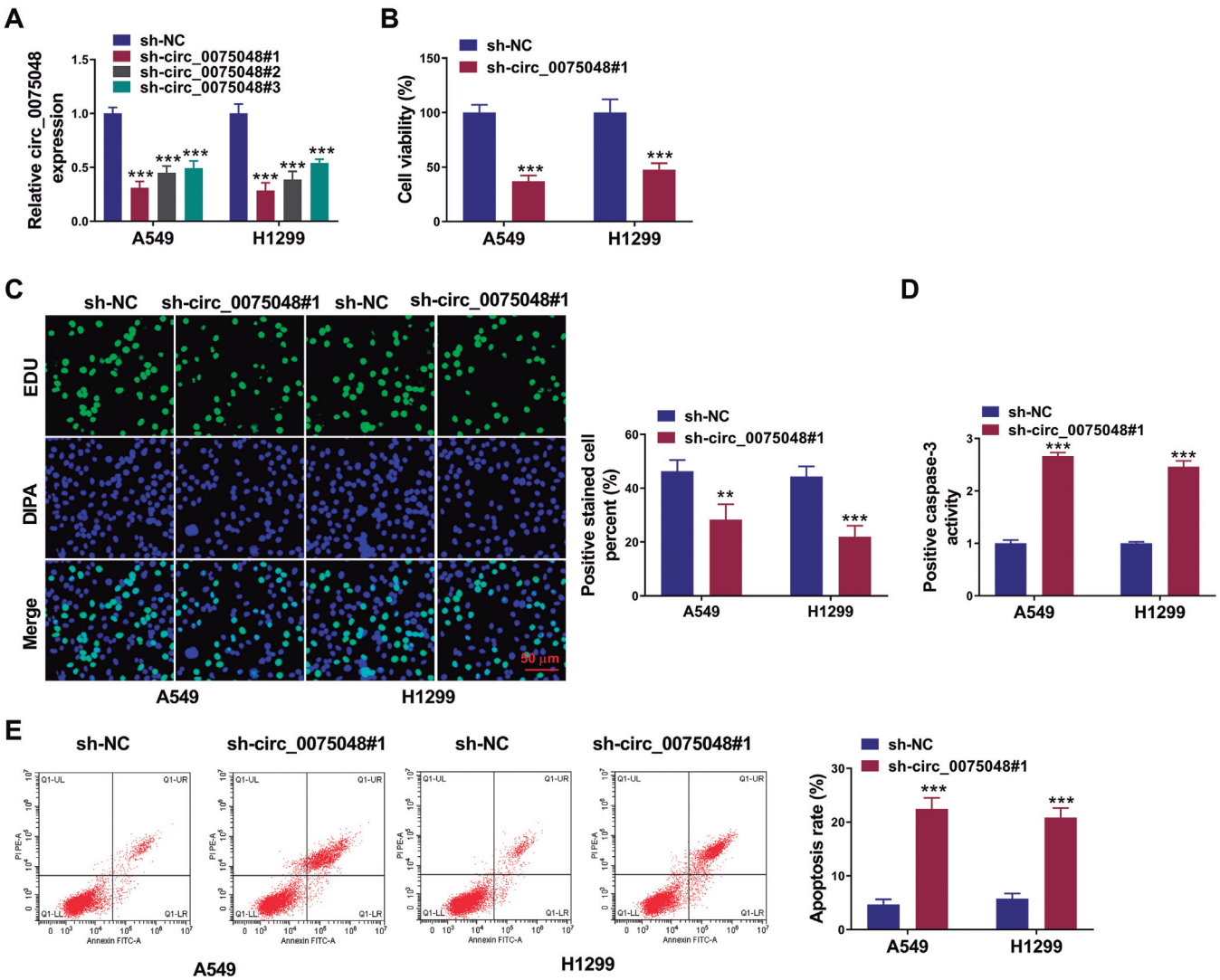

Fig. 2. Circ_0075048 silencing retarded the development of NSCLC cells. **A.** The inhibition efficiency of circ_0075048 knockdown on circ_0075048 in A549 and H1299 cells was detected by qRT-PCR. **B, C.** Cell viability and cell proliferation of A549 and H1299 cells were measured by CCK8 and EdU assays. **D, E.** The effect of circ_0075048 knockdown on cell apoptosis was estimated by caspase-3 activity and flow cytometry. ***P<0.001.

via qRT-PCR, the data exhibited that circ_0075048 was remarkably reduced in A549 and H1299 cells with circ_0075048 knockdown, among which the transfection efficiency of sh-circ_0075048#1 was the highest (Fig. 2A). Cell viability of A549 and H1299 cells was reduced by sh-circ_0075048#1 (Fig. 2B). EdU assay showed that

Table 3. Univariate and multivariate analysis for factors related to overall survival using the COX proportional hazard model.

Characteristics		Univariate analysis			Multivariate analysis	
		P	HR	95% CI	*P*	HR
Age	<50 vs. ≥50	0.4620	0.7680	0.3801-1.552	N.A	
Gender	Female vs. male	0.3569	0.7190	0.3564-1.451	N.A	
Tumor size	<5 vs. ≥5	0.0105	0.4393	0.2166-0.8911	N.A	
Histology	Adenoma vs. Squamous	0.0893	0.5421	0.2675-1.099	N.A	
Differentiation	Moderate-Poor vs. Well	0.1765	0.6138	0.3025-1.246	N.A	
TNM stage	I+II vs. III+IV	0.0001	0.2480	0.1222-0.5031	0.032	3.266
Lymph node metastasis	Absence vs. Presence	<0.0001	0.07042	0.03487-0.1422	0.001	5.273
Circ_0075048 expression	Low vs. High	0.0034	0.3422	0.1668-0.7020	0.053	2.279

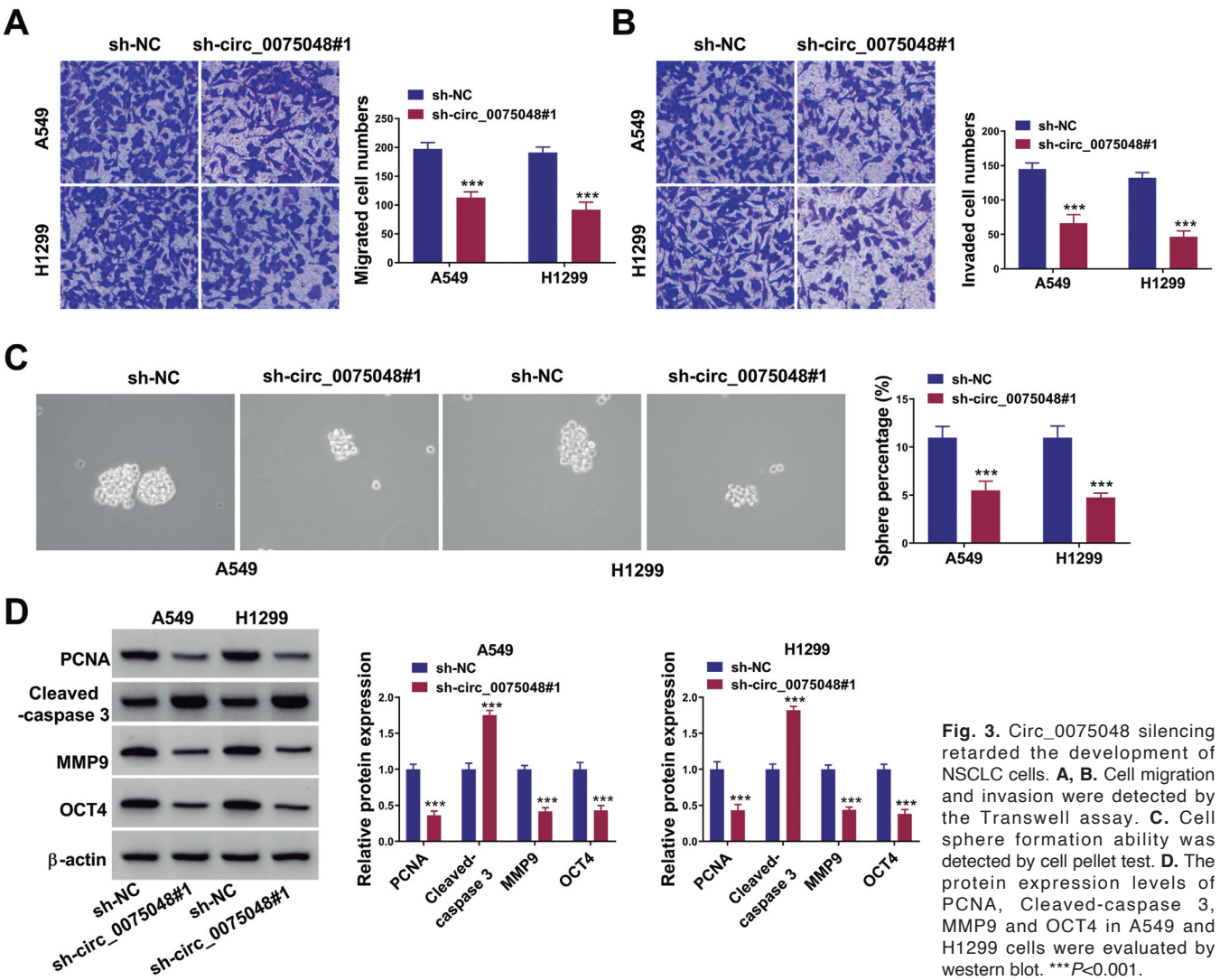

Fig. 3. Circ_0075048 silencing retarded the development of NSCLC cells. **A, B.** Cell migration and invasion were detected by the Transwell assay. **C.** Cell sphere formation ability was detected by cell pellet test. **D.** The protein expression levels of PCNA, Cleaved-caspase 3, MMP9 and OCT4 in A549 and H1299 cells were evaluated by western blot. ***P<0.001.

cell proliferation was inhibited in A5549 and H1299 cells with sh-circ_0075048#1 transfection (Fig. 2C). Sh-circ_0075048#1 induced cell apoptosis of A549 and H1299 cells, evidenced by decreased caspase-3 activity and apoptosis rate (Fig. 2D,E). Besides, silencing of circ_0075048 suppressed migrated and invaded cells (Fig. 3A,B) and sphere percentage (Fig. 3C). Western blot assay showed that the downregulation of circ_0075048 impaired the expression of PCNA, MMP9 and OCT4 (proliferation, invasion and stemness-related markers) in A549 and H1299 cells, while Cleaved-caspase 3 was reinforced in cells transfected with sh-circ_0075048#1 (Fig. 3D). Silencing of circ_0075048 suppressed the progress of NSCLC cells.

Circ_0075048 sponged miR-1225-5p in NSCLC cells

The data of qRT-PCR suggested that miR-1225-5p was down-regulated in NSCLC tissues, and was negatively correlated with circ_0075048 expression (Fig. 4A,B). Moreover, miR-1225-5p was decreased in NSCLC cells (Fig. 4C). The content of miR-1225-5p was increased in A549 and H1299 cells by miR-1225-5p overexpression (Fig. 4D). Based on circinteractome (https://circinteractome.nia.nih.gov/mirna_target_sites.html), miR-1225-5p was a target of circ_0075048 (Fig. 4E), and we verified this using dual-luciferase reporter assay, RNA-pull down experiment and RIP assay. Dual-luciferase reporter assay revealed that miR-1225-5p mimic reduced the luciferase activity of circ_0075048-WT rather than circ_0075048-MUT in A54 and H1299 cells (Fig. 4F). In addition, pull-down assay showed that circ_0075048 was captured by bio-miR-1225-5p (Fig. 4G). Moreover, both circ-MALAT1 and miR-512-5p were efficiently pulled down by anti-AGO2 antibodies compared with IgG (Fig. 4H). MiR-1225-5p expression was increased with circ_0075048 knockdown in A549 and H1299 cells (Fig. 4I). The data suggested that miR-1225-5p was downregulated in NSCLC, and was negatively regulated by circ_0075048.

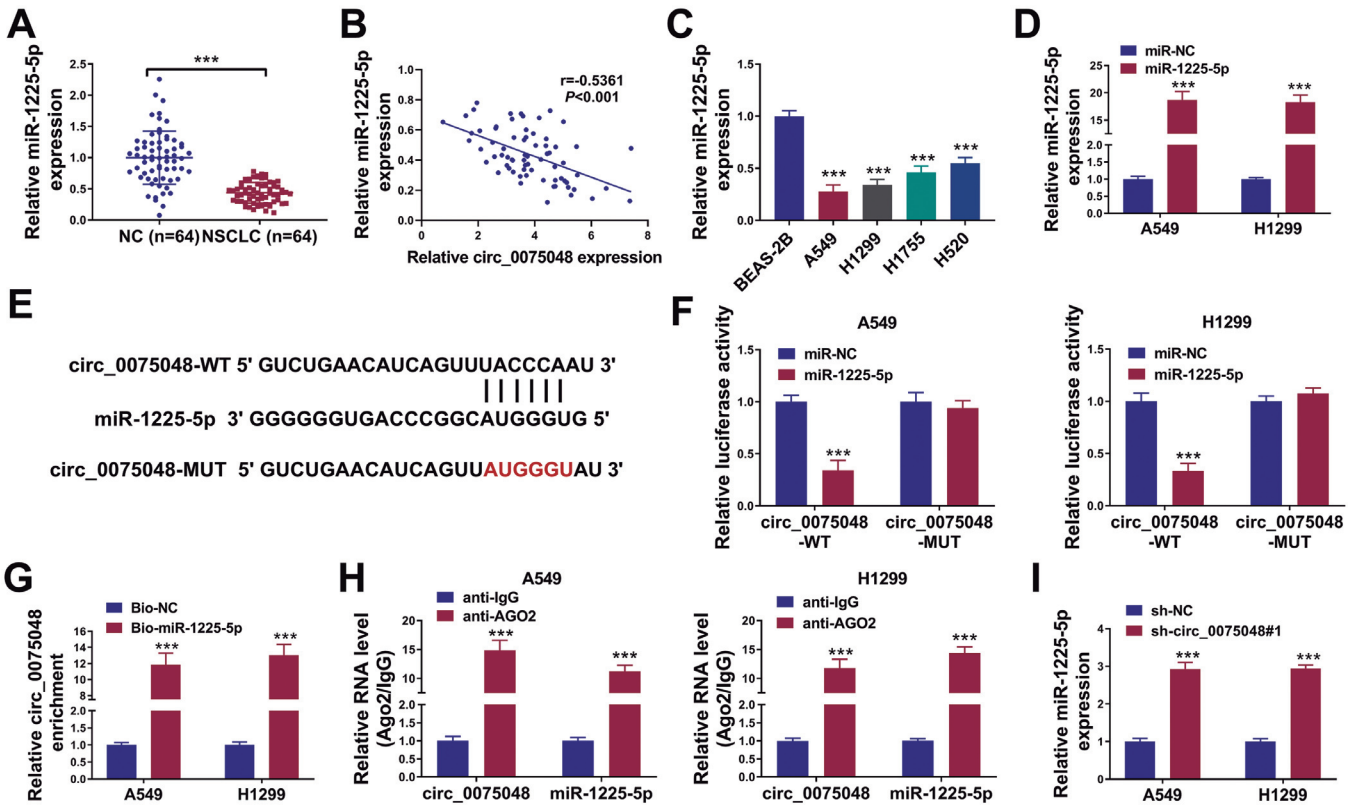

Fig. 4. MiR-1225-5p was regulated by circ_0075048 in NSCLC. **A.** MiR-1225-5p in NSCLC tissues and normal tissues was analyzed by qRT-PCR. **B.** Correlation analysis between circ_0075048 and miR-1225-5p expression was analyzed by Pearson's correlation analysis. **C, D.** QRT-PCR was used for testing miR-1225-5p expression. **E.** The binding sites between circ_0075048 and miR-1225-5p were predicted by Circinteractome. **F.** Dual-luciferase reporter assay was used for detecting luciferase activity. **G.** The ability of miR-1225-5p to pull down circ_0075048 was detected by RNA-pull down assay. **H.** RIP assays were performed to examine the levels of circ_0075048 and miR-1225-5p in A549 and H1299 cells. **I.** QRT-PCR was performed to analyze miR-1225-5p expression in A549 and H1299 cells. ***$P<0.001$.

Inhibition of miR-1225-5p partially reversed the effects of circ_0075048 knockdown on NSCLC cells

Then the function of miR-1225-5p in NSCLC was investigated. The level of miR-1225-5p was significantly diminished in A549 and H1299 cells with miR-1225-5p knockdown (Fig. 5A). Subsequently, we found that silencing of miR-1225-5p caused the enhancement of cell proliferation (Fig. 5B-C), inhibition of cell apoptosis (Fig. 5D,E), and promotion of cell migration, invasion and stemness (Fig. 5F-H) in A549 and H1299 cells. Furthermore, western blot analysis also showed that downregulation of miR-1225-5p up-regulated PCNA, MMP9 and OCT4 protein levels and reduced Cleaved-caspase 3 levels in A549 and H1299 cells (Fig. 5I).

Next, to assess whether miR-1255-5p mediated the functions caused by circ_0075048 in NSCLC cells, we performed rescue assays. Circ_0075048 knockdown led to an increase of miR-1225-5p levels, which were reversed by the introduction of miR-1225-5p inhibitor (Fig. 6A). Our results of CCK-8 and EdU analyses showed that sh-circ_0075048#1+anti-NC group exhibited reduced cell viability and proliferation compared with the sh-NC+anti-NC group, meanwhile, co-transfection of anti-miR-1225-5p and sh-circ_0075048#1 reversed this situation (Fig. 6B,C). With the co-transfection of anti-miR-1225-5p, the positive role of sh-circ_0075048#1 addition on apoptosis was significantly restored (Fig. 6D,E). The downregulation of miR-1225-5p impaired the inhibitory effects on cell migration, invasion and sphere formation caused by the circ_0075048 knockdown (Fig. 6F-H). The effects of sh-circ_0075048#1 on PCNA, Cleaved-caspase 3, MMP9 and OCT4 were overturned by miR-1225-5p blocking (Fig. 6I,J). In short, circ_0075048acted as a sponge and interacted with miR-1225-5p to regulate the evolution of NSCLC.

HMGB2 was negatively regulated by miR-1225-5p in NSCLC cells

The results of qRT-PCR elucidated that HMGB2 was upregulated in NSCLC tissues (Fig. 7A), which was negatively correlated with miR-1225-5p (Fig. 7B).

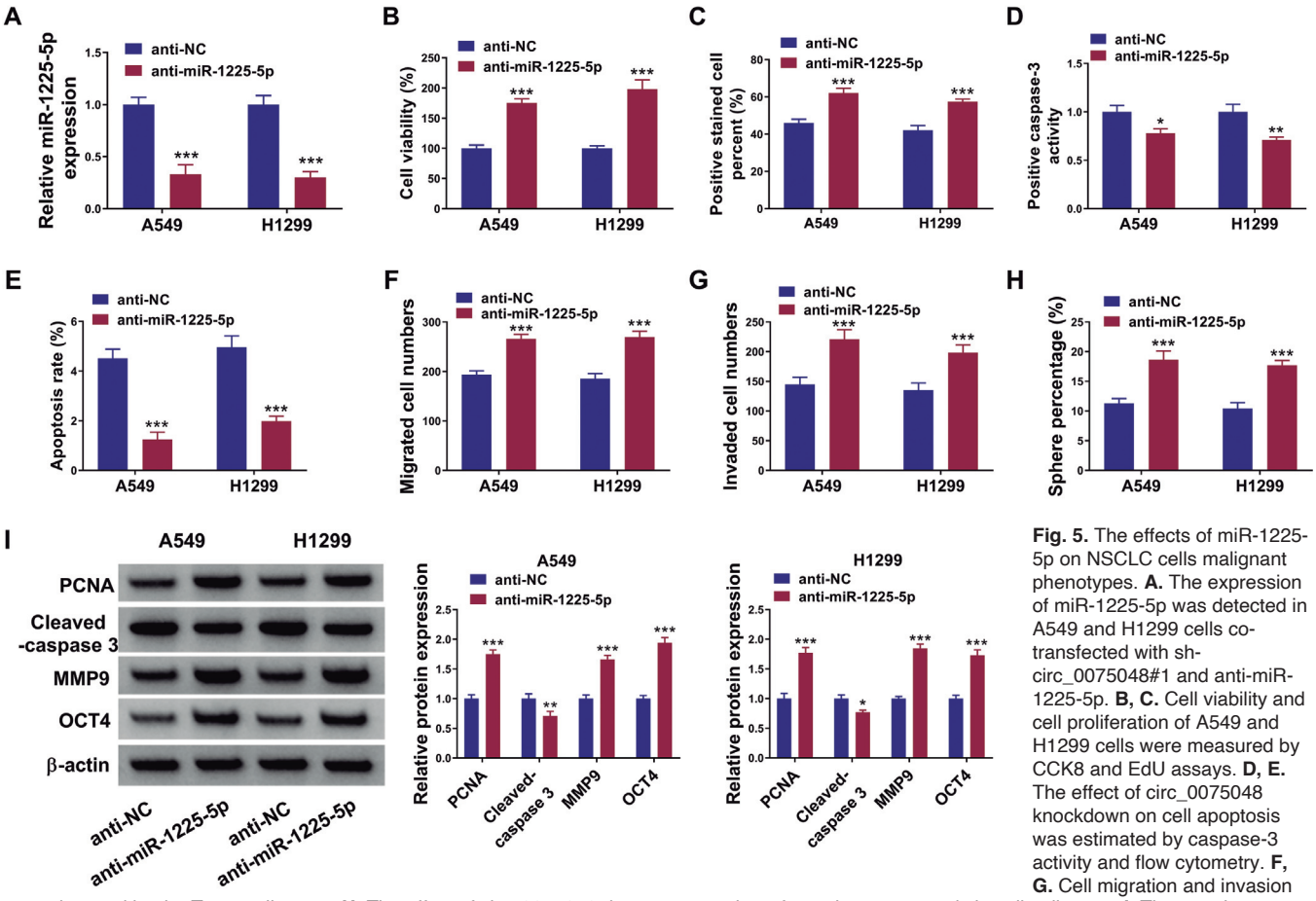

Fig. 5. The effects of miR-1225-5p on NSCLC cells malignant phenotypes. **A.** The expression of miR-1225-5p was detected in A549 and H1299 cells co-transfected with sh-circ_0075048#1 and anti-miR-1225-5p. **B, C.** Cell viability and cell proliferation of A549 and H1299 cells were measured by CCK8 and EdU assays. **D, E.** The effect of circ_0075048 knockdown on cell apoptosis was estimated by caspase-3 activity and flow cytometry. **F, G.** Cell migration and invasion were detected by the Transwell assay. **H.** The effect of circ_0075048 decrease on sphere formation was tested via cell pellet test. **I.** The protein expression levels of PCNA, Cleaved-caspase 3, MMP9 and OCT4 in A549 and H1299 cells were evaluated by western blot. **P*<0.05, ***P*<0.01, ****P*<0.001.

Moreover, IHC assay and western blot also showed that HMGB2 was upregulated in NSCLC cells (Fig. 7C,D). Based on starBase (https://starbase.sysu.edu.cn/), the binding sites of miR-1225-5p and HMGB2 are shown in Fig. 7E. Overexpression of miR-1225-5p inhibited the luciferase activity in A549 and H1299 cells with HMGB2-3'UTR-WT. After mutation in the predicted HMGB2-3'UTR binding sites, its inhibitory function disappeared (Fig. 7F). And HMGB2 was negatively regulated by miR-1225-5p (Fig. 7G-H). Anti-miR-1225-5p reversed the effect of sh-circ_0075048#1 introduction on HMGB2 expression in A549 and H1299 cells (Fig. 7I). In summary, circ_0075048 acted as a sponge of miR-1225-5p to regulate the expression of HMGB2 in NSCLC cells.

Overexpression of HMGB2 overturned the effects of miR-1225-5p on NSCLC cells

The expression level of HMGB2 was obviously multiplied after HMGB2 was overexpressed by western blot assay (Fig. 8A). Then the function of HMGB2 in NSCLC cells was evaluated. It was found that HMGB2 up-regulation promoted cell proliferation (Fig. 8B and C), suppressed cell apoptosis (Fig. 8D,E), and induced cell migration and invasion (Fig. 8F,G) as well as enhancing cell sphere percentage (Fig. 8H) in A549 and H1299 cells. Moreover, the levels of PCNA, MMP9 and OCT4 protein were increased and Cleaved-caspase 3 protein levels were reduced after HMGB2 up-regulation in A549 and H1299 cells (Fig. 8I).

Thereafter, rescue assays were conducted. As shown in Fig. 9A, overexpression of HMGB2 did not influence the expression of miR-1225-5p. Functionally, overexpression of miR-1225-5p repressed cell viability and proliferation of A549 and H1299 cells, while HMGB2 upregulation reversed these effects (Fig. 9B,C). The promotion effect of miR-1225-5p on apoptosis was reversed after HMGB2 co-transfection (Fig. 9D,E). HMGB2 alleviated the suppressive effects of miR-1225-

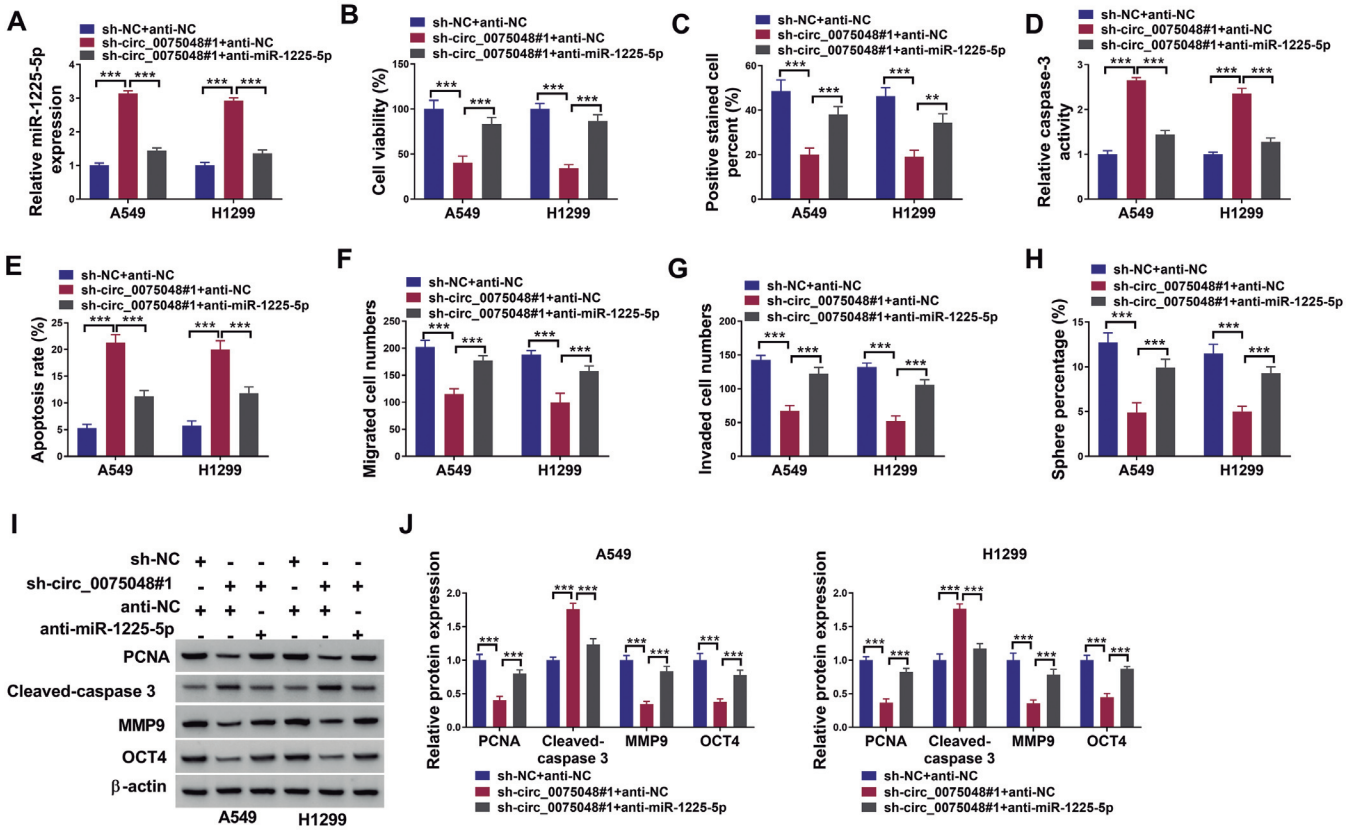

Fig. 6. Downregulation of miR-1225-5p mitigated the effects of circ_0075048 knockdown of A549 and H1299 cells. **A.** MiR-1225-5p expression in A549 and H1299 cells was detected by qRT-PCR after anti-miR-1225-5p was transfected. **B-J.** A549 and H1299 cells were co-transfected with sh-NC and anti-NC, sh-circ_0075048#1 and anti-NC or sh-circ_0075048#1 and anti-miR-1225-5p. **B, C.** Cell viability and proliferation were measured using CCK8 and EdU assays. **D, E.** The apoptosis of A549 and H1299 cells was tested by caspase-3 activity and flow cytometry. **F, G.** Transwell assay was used to assess cell migration and invasion. **H.** The capability of sphere formation was determined by cell pellet assay. **I, J.** Western blot was carried out for measuring the protein expression of PCNA, Cleaved-caspase 3, MMP9 and OCT4 in A549 and H1299 cells. ***P<0.001.

5p overexpression on cell migration, invasion and sphere formation in A549 and H1299 cells (Fig. 9F-H). The effects of miR-1225-5p on PCNA, Cleaved-caspase 3, MMP9 and OCT4 were overturned by HMGB2 increase (Fig. 9I,J). The data indicated that the effects of miR-1225-5p on NSCLC cells growth were abolished by HMGB2 upregulation.

Circ_0075048 silence suppressed tumor growth in vivo

For the purpose of proving the function of circ_0075048 *in vivo*, sh-circ_0075048#1 or sh-NC transfected A549 cells were applied to establish tumor xenograft mice models. The volume and weight of tumors in sh-circ_0075048#1 group were markedly decreased in comparison to the sh-NC group (Fig. 10A,B). In addition, Ki-67 and HMGB2 levels were obviously lowered in sh-circ_0075048#1 group (Fig. 10C). The mice tumor tissues with silenced circ_0075048 presented lower expression of circ_0075048, and higher expression of miR-1225-5p (Fig. 10D). Western blot results showed that HMGB2, PCNA, MMP9 and OCT4 expression in sh-circ_0075048#1 tumor tissues were obviously decreased, while Cleaved-caspase 3 level was intensified (Fig. 10E), and the increased Cleaved-caspase 3 protein was also confirmed by IHC analysis (Fig. 10F). Altogether, these results disclosed that

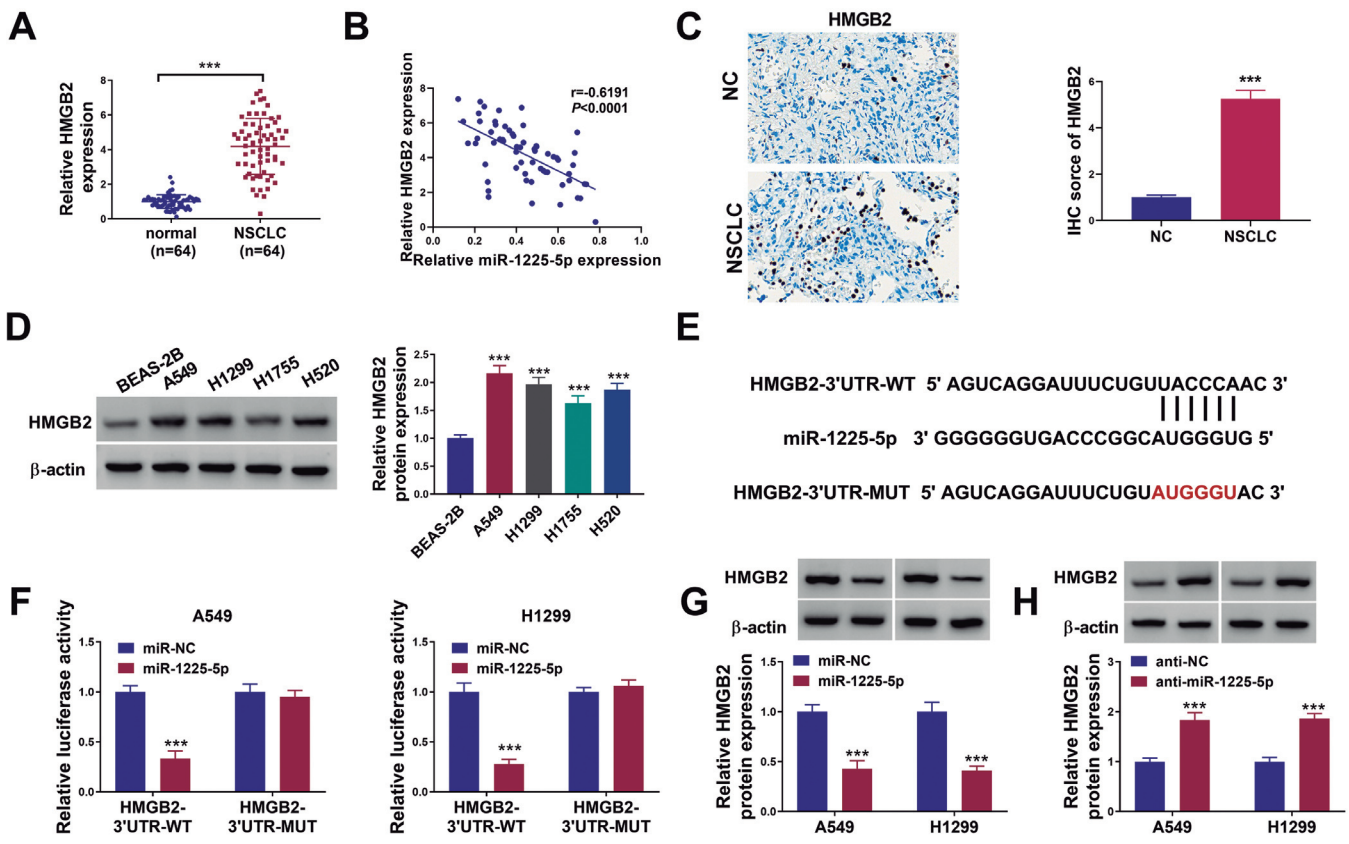

Fig. 7. MiR-1225-5p regulated HMGB2 expression in NSCLC. **A.** QRT-PCR for HMGB2 expression in NSCLC tissues. **B.** Correlation analysis between HMGB2 and miR-1225-5p expression was analyzed by Pearson's correlation analysis. **C.** IHC analysis of HMGB2 protein expression in NSCLC tissues. **D.** Western blot was carried for testing HMGB2 expression in NSCLC cells. **E.** Target sites of miR-1225-5p in HMGB2 were screened by StarBase. **F.** The luciferase activity was assessed at 48 h after transfection. **G, H.** The content of HMGB2 in A549 and H1299 cells was tested by western blot assay after transfection with miR-1225-5p or anti-miR-1225-5p. **I.** HMGB2 expression was detected by western blot after sh-NC+anti-NC, sh-circ_0075048#1+anti-NC or sh-circ_0075048#1+anti-miR-1225-5p were transfected into A549 and H1299 cells. ***P<0.001.

circ_0075048 silencing curbed the tumor growth *in vivo*.

Discussion

Lung cancer was reported to be responsible for one quarter of deaths in the United States in 2019 (Siegel and Miller, 2019). NSCLC, the most common form of lung cancer, has a low five-year survival rate (Chen et al., 2014; Inamura, 2018). In this study, we showed that circ_0075048 played an important role in NSCLC by regulating miR-1225-5p and HMGB2.

CircRNAs are a kind of non-coding RNAs formed by reverse splicing in non-classical splicing methods (Guo et al., 2018). CircRNAs have stable covalent closed circular structures and play a role in many biological functions (Zhu et al., 2019). Wang et al. showed that circ-IGF1R was prominently retarded in lung cancer tissues, which inhibited invasion and migration, and was associated with lymph node metastasis (Xu et al., 2020). Zhu et al. identified that hsa-circ-0049271, hsa-circ-0009150 and other circRNAs in NSCLC were associated with the diagnosis of NSCLC (Zhu et al., 2021). By analyzing GSE158695, we showed that circ_0075048 was significantly overexpressed in lung cancer tissues and located in cytoplasm with a stable ring structure, and silencing of circ_0075048 reduced cell proliferation, migration, invasion and sphere formation, and induced cell apoptosis. Circ_0075048 knockdown suppressed tumor growth *in vivo*. In addition, the protein levels of PCNA, MMP9 and OCT4 were reduced after circ_0075048 down-regulation, and Cleaved-caspase 3 expression was aberrantly increased by circ_0075048 knockdown. The data indicated that circ_0075048 accelerated the growth of NSCLC.

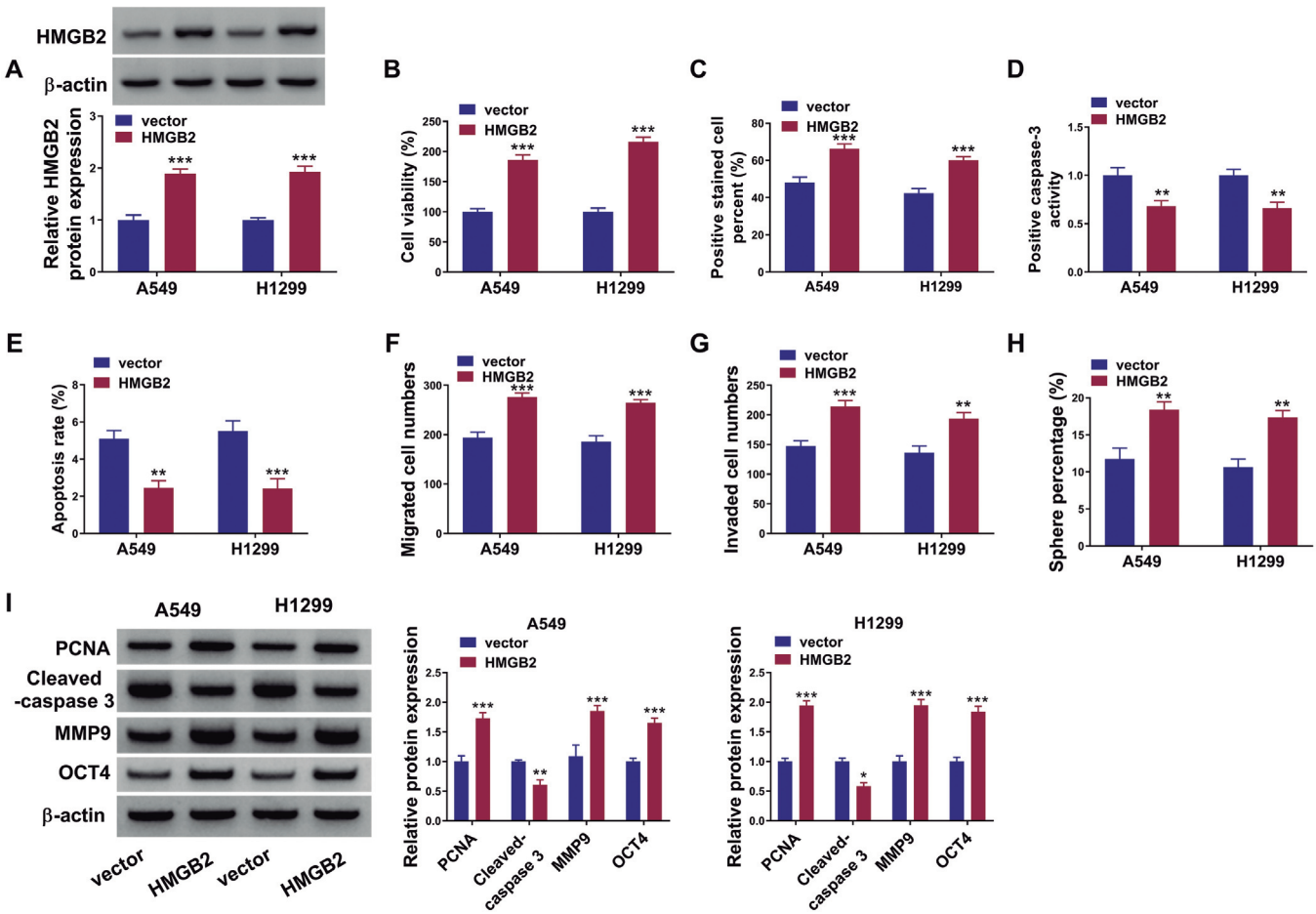

Fig. 8. The effects of HMGB2 on NSCLC cells malignant phenotypes. **A.** Western blot was utilized to determine the expression of HMGB2 after transfection with vector or HMGB2 in A549 and H1299 cells. **B, C.** Cell viability and cell proliferation of A549 and H1299 cells were measured by CCK8 and EdU assays. **D, E.** The effect of circ_0075048 knockdown on cell apoptosis was estimated by caspase-3 activity and flow cytometry. **F, G.** Cell migration and invasion were detected by the Transwell assay. **H.** The effect of circ_0075048 decrease on sphere formation was tested via cell pellet test. **I.** The protein expression levels of PCNA, Cleaved-caspase 3, MMP9 and OCT4 in A549 and H1299 cells were evaluated by western blot. **P*<0.05, ***P*<0.01, ****P*<0.001.

CircRNA mainly distributed in the cytoplasm can act as a miRNA sponge to perform its effects (Arnaiz et al., 2019). Circinteractome was performed to predict the targets of circ_0075048, and miR-1225-5p was screened to be the target of circ_0075048. MiR-1225-5p was discovered to be associated with various cancers, like osteosarcoma (Zhang et al., 2020), hepatocellular carcinoma (Liu et al., 2020; Zhang et al., 2022) and colorectal cancer (Yang et al., 2021). We showed that miR-1225-5p was specially confined in NSCLC tissues and cells, and was negatively regulated via circ_0075048. The results of functional rescue experiments suggested that the effects of circ_0075048 silencing on cell proliferation, apoptosis, migration, invasion and sphere formation were restored by miR-1225-5p knockdown. Also, overexpression of miR-1225-5p restrained cell proliferation, migration, invasion and sphere formation, and promoted cell apoptosis in NSCLC, and these outcomes were consistent with the findings of Li et al. (2020), who demonstrated that miR-1225-5p was drastically curbed in NSCLC tissues, and was a potential prognostic factor in NSCLC. To sum up, circ_0075048 facilitated the progression of NSCLC by regulating miR-1225-5p.

CircRNAs had been reported to be involved in cancer treatment and prognosis by regulating the expression of downstream genes of miRNAs through sponging miRNAs (Chen et al., 2018). HMGB2 was found to be the downstream gene for miR-1225-5p by starBase in this study. It was reported that HMGB2 was upregulated in NSCLC (Lou et al., 2022) and involved in the growth and development of NSCLC (Li et al., 2018). HMGB2 was intensified in NSCLC tissues and cells in our research, and was negatively regulated via miR-1225-5p. The repressive effect of circ_0075048 depletion on HMGB2 expression was overturned by miR-1225-5p decrease. At the same time, overexpression of HMGB2 ameliorated the effects of miR-1225-5p upregulation on cell proliferation, apoptosis, migration, invasion and sphere formation in NSCLC

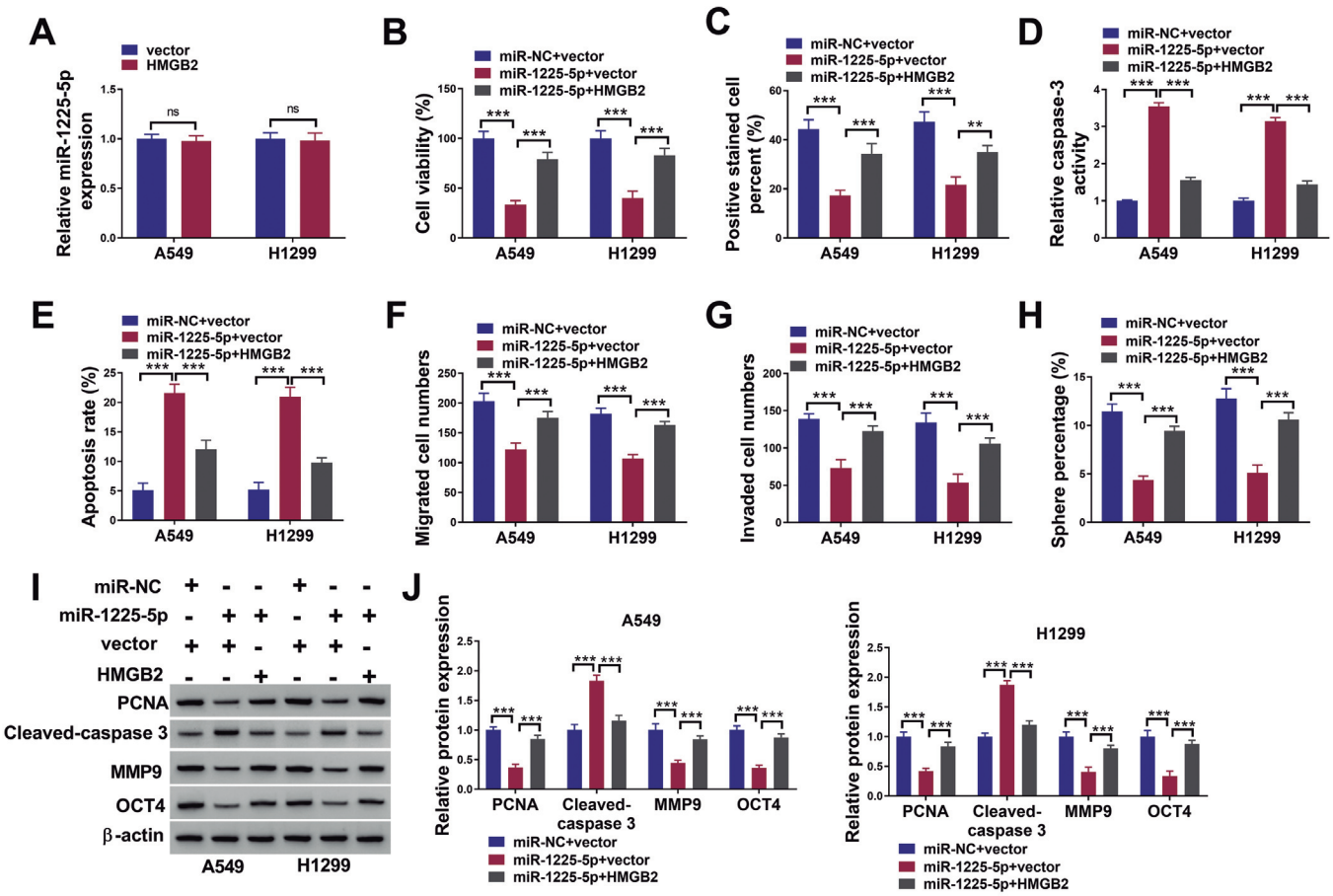

Fig. 9. MiR-1225-5p regulated the growth of NSCLC cells by regulating HMGB2. **A.** The expression of miR-1225-5p after HMGB2 overexpression in A549 and H1299 cells. **B-J.** Cell viability **(B)**, proliferation **(C)**, apoptosis **(D, E)**, migration **(E)**, invasion **(F)**, sphere formation **(G)** and the protein expression of PCNA, Cleaved-caspase 3, MMP9 and OCT4 **(H, I)** were tested by CCK8 assay **(B)**, EdU assay **(C)**, caspase-3 activity analysis **(D)**, flow cytometry **(E)**, transwell assay **(F, G)**, cell pellet assay **(H)** and western blot assay **(I, J)** in A549 and H1299 cells transfected with miR-NC+vector, miR-1225-5p+vector or miR-1225-5p+HMGB2. ***P<0.001.

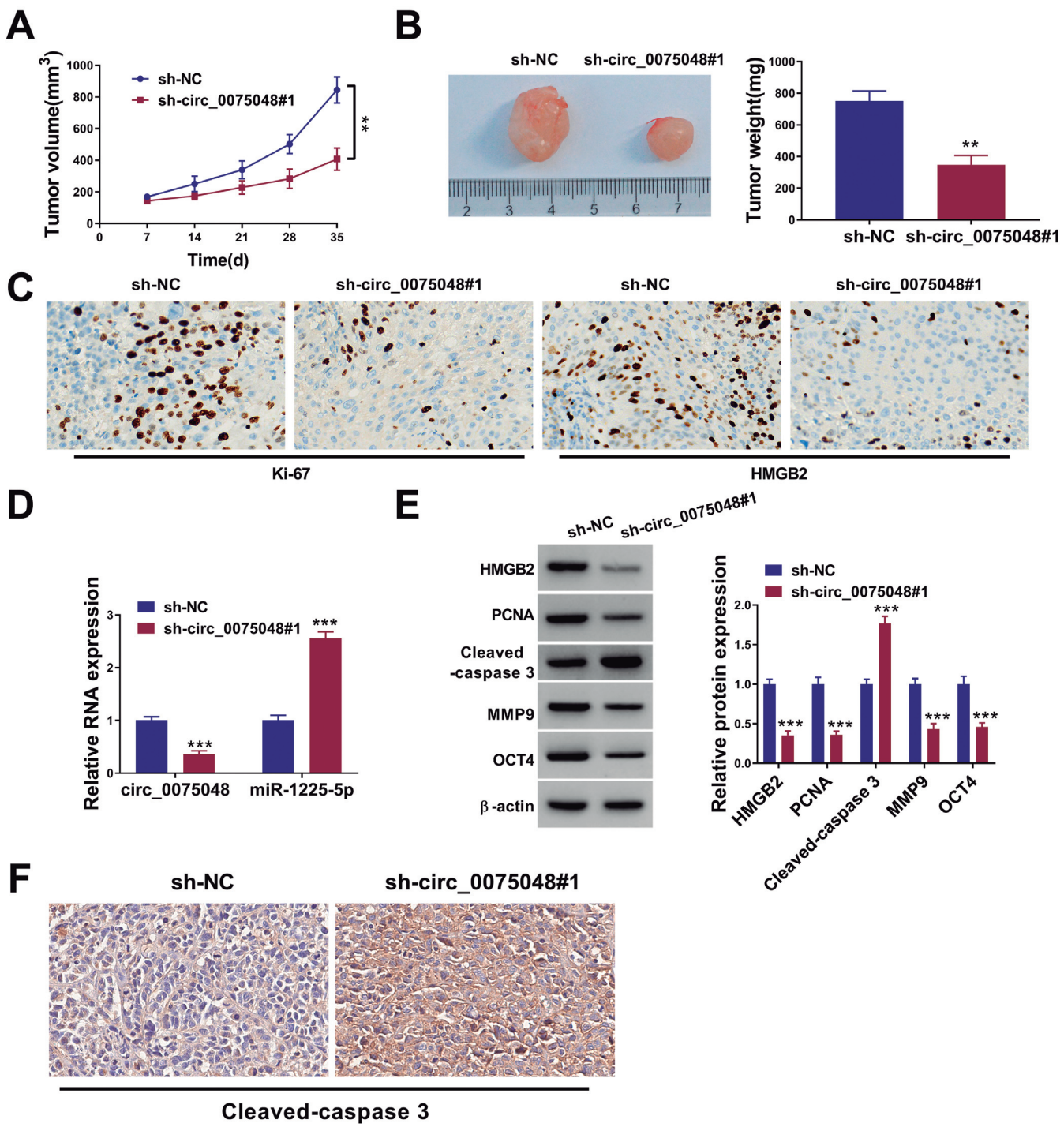

Fig. 10. Silencing of circ_0075048 constrained tumor growth *in vivo*. **A.** Tumor volume was detected every 7 days. **B.** Tumor weight in sh-NC and sh-circ_0075048#1 was determined. **C.** IHC was used for analyzing the expression of Ki-67 and HMGB2 in tumor tissues. **D.** QRT-PCR was carried out for measuring the contents of circ_0075048 and miR-1225-5p. **E.** HMGB2, PCNA, Cleaved-caspase 3, MMP9 and OCT4 protein expression in tissues were evaluated by western blot assay. **F.** IHC was used for analyzing the expression of Cleaved-caspase3 in tumor tissues. $^{**}P<0.01$, $^{***}P<0.001$.

cells. In a word, circ_0075048 regulated cell growth though the miR-1225-5p/HMGB2 axis in NSCLC.

Conclusion

In this study, it was found that circ_0075048 was enhanced in NSCLC tissues and cells, and involved in the malignant growth and poor prognosis of NSCLC. The data of function rescue experiments disclosed that circ_0075048 regulated the progression of NSCLC through the miR-1225-5p/HMGB2 axis.

Data Availability Statement. The data sets used and/or analyzed during the current study are available from the corresponding author on reasonable request.

Conflict of interest. The authors report no conflicts of interest in this work.

Funding. None.

References

Arnaiz E., Sole C., Manterola L., Iparraguirre L., Otaegui D. and Lawrie C.H. (2019). CircRNAs and cancer: Biomarkers and master regulators. Semin. Cancer Biol. 58, 90-99.

Chaudhuri K. and Chatterjee R. (2007). MicroRNA detection and target prediction: Integration of computational and experimental approaches. DNA Cell Biol. 26, 321-337.

Chen Z., Fillmore C.M., Hammerman P.S., Kim C.F. and Wong K.K. (2014). Non-small-cell lung cancers: a heterogeneous set of diseases. Nat. Rev. Cancer 14, 535-546.

Chen D., Ma W., Ke Z. and Xie F. (2018). CircRNA hsa_circ_100395 regulates miR-1228/TCF21 pathway to inhibit lung cancer progression. Cell Cycle 17, 2080-2090.

Chen J., Tan Y., Sun F., Hou L., Zhang C., Ge T., Yu H., Wu C., Zhu Y., Duan L., Wu L., Song N., Zhang L., Zhang W., Wang D., Chen C., Wu C., Jiang G. and Zhang P. (2020). Single-cell transcriptome and antigen-immunoglobin analysis reveals the diversity of B cells in non-small cell lung cancer. Genome Biol. 21, 152.

Fang J., Ge X., Xu W., Xie J., Qin Z., Shi L., Yin W., Bian M. and Wang H. (2020). Bioinformatics analysis of the prognosis and biological significance of HMGB1, HMGB2, and HMGB3 in gastric cancer. J. Cell. Physiol. 235, 3438-3446.

Forde P.M., Chaft J.E., Smith K.N., Anagnostou V., Cottrell T.R. and Hellmann M.D. (2018). Neoadjuvant PD-1 blockade in resectable lung cancer. N. Engl. J. Med. 378, 1976-1986.

Fu D., Li J., Wei J., Zhang Z., Luo Y., Tan H. and Ren C. (2018). HMGB2 is associated with malignancy and regulates Warburg effect by targeting LDHB and FBP1 in breast cancer. Cell Commun. Signal. 16, 8.

Guo S.J., Zeng H.X., Huang P., Wang S., Xie C.H. and Li S.J. (2018). MiR-508-3p inhibits cell invasion and epithelial-mesenchymal transition by targeting ZEB1 in triple-negative breast cancer. Eur. Rev. Med. Pharmacol. Sci. 22, 6379-6385.

Hong W., Xue M., Jiang J., Zhang Y. and Gao X. (2020). Circular RNA circ-CPA4/ let-7 miRNA/PD-L1 axis regulates cell growth, stemness, drug resistance and immune evasion in non-small cell lung cancer (NSCLC). J. Exp. Clin. Cancer Res. 39, 149.

Inamura K. (2018). Update on immunohistochemistry for the diagnosis of lung cancer. Cancers (Basel) 10, 72.

Jiao J., Zhang T., Jiao X., Huang T., Zhao L., Ma D. and Cui B. (2020). hsa_circ_0000745 promotes cervical cancer by increasing cell proliferation, migration, and invasion. J. Cell. Physiol. 235, 1287-1295.

Li S., Yang J., Xia Y., Fan Q. and Yang K.P. (2018). Long noncoding RNA NEAT1 promotes proliferation and invasion via targeting miR-181a-5p in non-small cell lung cancer. Oncol. Res. 26, 289-296.

Li B., Zhang F. and Li H. (2020). miR-1225-5p inhibits non-small cell lung cancer cell proliferation, migration and invasion, and may be a prognostic biomarker. Exp. Ther. Med. 20, 172.

Liu L., Zhang W., Hu Y., Ma L. and Xu X. (2020). Downregulation of miR-1225-5p is pivotal for proliferation, invasion, and migration of HCC cells through NFκB regulation. J. Clin. Lab. Anal. 34, e23474.

Livak K.J. and Schmittgen T.D. (2001). Analysis of relative gene expression data using real-time quantitative PCR and the 2(-Delta Delta C(T)) method. Methods 25, 402-408.

Lou N., Zhu T., Qin D., Tian J. and Liu J. (2022). High-mobility group box 2 reflects exacerbated disease characteristics and poor prognosis in non-small cell lung cancer patients. Ir. J. Med. Sci. 19, 155-162.

Planchard D., Popat S., Kerr K., Novello S., Smit E.F., Faivre-Finn C., Mok T.S., Reck M., Van Schil P.E., Hellmann M.D. and Peters S. (2018). Metastatic non-small cell lung cancer: ESMO Clinical Practice Guidelines for diagnosis, treatment and follow-up. Ann. Oncol. 29, iv192-iv237.

Siegel R.L. and Miller K.D. (2019). Cancer statistics, 2019. CA Cancer J. Clin. 69, 7-34.

Sun P., Zhang D., Huang H., Yu Y., Yang Z., Niu Y. and Liu J. (2019). MicroRNA-1225-5p acts as a tumor-suppressor in laryngeal cancer via targeting CDC14B. Biol. Chem. 400, 237-246.

Tutar Y. (2014). miRNA and cancer; computational and experimental approaches. Curr. Pharm. Biotechnol. 15, 429.

Wang L., Tong X., Zhou Z., Wang S., Lei Z., Zhang T., Liu Z., Zeng Y., Li C., Zhao J., Su Z., Zhang C., Liu X., Xu G. and Zhang H.T. (2018). Circular RNA hsa_circ_0008305 (circPTK2) inhibits TGF-β-induced epithelial-mesenchymal transition and metastasis by controlling TIF1γ in non-small cell lung cancer. Mol. Cancer 17, 140.

Wang G.H., Wang L.Y., Zhang C., Zhang P., Wang C.H. and Cheng S. (2020). MiR-1225-5p acts as tumor suppressor in glioblastoma via targeting FNDC3B. Open Med. (Wars) 15, 872-881.

Xu Z., Xiang W., Chen W., Sun Y., Qin F., Wei J., Yuan L., Zheng L. and Li S. (2020). Circ-IGF1R inhibits cell invasion and migration in non-small cell lung cancer. Thorac. Cancer 11, 875-887.

Yang K., Shen Z., Zou Y. and Gao K. (2021). Rosmarinic acid inhibits migration, invasion, and p38/AP-1 signaling via miR-1225-5p in colorectal cancer cells. J. Recept Signal Transduct. Res. 41, 284-293.

Zhang W., Wei L., Sheng W., Kang B., Wang D. and Zeng H. (2020). miR-1225-5p functions as a tumor suppressor in osteosarcoma by targeting Sox9. DNA Cell Biol. 39, 78-91.

Zhang D., Zhang Y., Zhang X., Zhai H., Sun X. and Li Y. (2022). Circ_0091579 serves as a tumor-promoting factor in hepatocellular carcinoma through miR-1225-5p/PLCB1 axis. Dig. Dis. Sci. 67, 585-597.

Zhou G.H., Lu Y.Y., Xie J.L., Gao Z.K., Wu X.B., Yao W.S. and Gu W.G. (2019). Overexpression of miR-758 inhibited proliferation, migration, invasion, and promoted apoptosis of non-small cell lung cancer cells

by negatively regulating HMGB. Biosci. Rep. 39, BSR20180855.
Zhu L., Liu Y., Yang Y., Mao X.M. and Yin Z.D. (2019). CircRNA ZNF609 promotes growth and metastasis of nasopharyngeal carcinoma by competing with microRNA-150-5p. Eur. Rev. Med. Pharmacol. Sci. 23, 2817-2826.
Zhu P., Huang H., Gu S., Liu Z., Zhang X., Wu K., Lu T., Li L., Dong C., Zhong C. and Zhou Y. (2021). Long noncoding RNA FAM225A promotes esophageal squamous cell carcinoma development and progression via sponging microRNA-197-5p and upregulating NONO. J. Cancer 12, 1073-1084.

Accepted November 23, 2022